Hydrologic conditions controlling runoff generation immediately after wildfire

Brian A. Ebel,[1] John A. Moody,[1] and Deborah A. Martin[1]

Received 30 September 2011; revised 6 February 2012; accepted 20 February 2012; published 30 March 2012.

[1] We investigated the control of postwildfire runoff by physical and hydraulic properties of soil, hydrologic states, and an ash layer immediately following wildfire. The field site is within the area burned by the 2010 Fourmile Canyon Fire in Colorado, USA. Physical and hydraulic property characterization included ash thickness, particle size distribution, hydraulic conductivity, and soil water retention curves. Soil water content and matric potential were measured indirectly at several depths below the soil surface to document hydrologic states underneath the ash layer in the unsaturated zone, whereas precipitation and surface runoff were measured directly. Measurements of soil water content showed that almost no water infiltrated below the ash layer into the near-surface soil in the burned site at the storm time scale (i.e., minutes to hours). Runoff generation processes were controlled by and highly sensitive to ash thickness and ash hydraulic properties. The ash layer stored from 97% to 99% of rainfall, which was critical for reducing runoff amounts. The hydrologic response to two rain storms with different rainfall amounts, rainfall intensity, and durations, only ten days apart, indicated that runoff generation was predominantly by the saturation-excess mechanism perched at the ash-soil interface during the first storm and predominantly by the infiltration-excess mechanism at the ash surface during the second storm. Contributing area was not static for the two storms and was 4% (saturation excess) to 68% (infiltration excess) of the catchment area. Our results showed the importance of including hydrologic conditions and hydraulic properties of the ash layer in postwildfire runoff generation models.

Citation: Ebel, B. A., J. A. Moody, and D. A. Martin (2012), Hydrologic conditions controlling runoff generation immediately after wildfire, *Water Resour. Res.*, *48*, W03529, doi:10.1029/2011WR011470.

1. Introduction

[2] In the last 30 years, the incidence of large wildfires and duration of the wildfire season in the forests of the western USA have increased [*Westerling et al.*, 2006]. For the northern Rocky Mountains in the USA, recent wildfire increases have been attributed to earlier snowmelt, which results in a longer season of potential fire ignition and overall drier fuel conditions [*Westerling et al.*, 2006]. Wildfire synchrony and frequency are forecast to increase in response to changes in global climate [*Kitzberger et al.*, 2007; *Pechony and Shindell*, 2010]. Reservoir storage for water supply can decrease from floods following wildfires [*Moody and Martin*, 2001a]. Water quality is also detrimentally affected after wildfires, which can increase heavy metal and nutrient concentrations and alter organic matter composition [*Gresswell*, 1999; *Smith et al.*, 2011; *Emelko et al.*, 2011]. The postwildfire impacts on drinking water quality and quantity can include substantial increases in runoff and accompanying sediment yield following wildfire [e.g., *Prosser and Williams*, 1998; *Moody and Martin*, 2001a, 2001b]. Advancing knowledge of wildfire impacts on soil physical and hydraulic properties, hydrologic states, and runoff generation is a timely research topic in light of increases in wildfire frequency and severity in the western USA considering the potential loss of human life from natural hazards, damage to the built environment, and impairment of ecosystems and water resources by wildfire [e.g., *Neary et al.*, 1999; *Cannon et al.*, 2001].

[3] Wildfire changes the hydrology of forest ecosystems by removing the forest canopy and litter/duff layers, reducing organic content in soils, producing ash (a mixture of black carbon, soot, charred material, charcoal, and mineral material [*Moody et al.*, 2009]), enhancing the impact of hydrophobic substances [e.g., *Robichaud et al.*, 2000], and changing soil physical and hydraulic properties [e.g., *Certini*, 2005]. These changes vary in space and temporal duration depending on vegetation, climate, and wildfire severity. Wildfire impacts on physical and hydraulic properties of soil, in addition to changes in hydrologic states (e.g., soil water content and matric potential), can change how catchments generate runoff [e.g., *Ice et al.*, 2004; *Shakesby and Doerr*, 2006]. Comprehension of how wildfire affects physical and hydraulic properties and hydrologic states, which in turn may control runoff generation, is minimal, especially in the few months immediately after a wildfire. Of

[1]U.S. Geological Survey, National Research Program, Boulder, Colorado, USA.

This paper is not subject to U.S. copyright.
Published in 2012 by the American Geophysical Union

particular importance is the role of ash in runoff generation, which has been examined extensively at plot scales [e.g., *Cerdà and Doerr*, 2008; *Gabet and Sternberg*, 2008; *Onda et al.*, 2008; *Woods and Balfour*, 2008], but almost no studies have considered the catchment scale [*Campbell et al.*, 1977].

[4] The principal objectives of this study are to examine: (1) wildfire effects on physical and hydraulic properties of soil and hydrologic states, (2) how these properties and states control postwildfire runoff generation mechanisms, and (3) the role of ash in controlling runoff. We focus on the period immediately after the wildfire was extinguished through the first few precipitation events when an ash layer was present. Continuous and event-driven (i.e., rainstorm) analyses are used because continuous hydrologic processes operating over day to week time scales produce initial conditions for runoff events at minute to hour scales. Our work provides unique insight into the surface and subsurface hydrologic conditions that control postwildfire runoff generation.

2. Fourmile Canyon Wildfire and Hillslope Field Sites

2.1. Regional Setting

[5] The field site is in the Front Range Foothills in Colorado (CO), USA, near the city of Boulder (Figure 1). Elevations within the burn perimeter range from 1940 to 2620 m. It is in a semiarid climate that is strongly continental. Annual precipitation in this area is approximately 500 mm within the Fourmile Canyon area, based on the 20-year period of record at the nearby (~4 km away) Sugarloaf site (NADP site CO94 at 39.99 N, −105.48 W; National Atmospheric Deposition Program, http://nadp.sws.uiuc.edu/data/; accessed 22 June 2011). Maximum precipitation is in April or May from cyclonic storms (low intensity, long duration) with a secondary peak in July and August [*Peet*, 1981] associated with the North American monsoon convective storms (high intensity, short duration) [*Douglas et al.*, 2004]. High rainfall intensities (e.g., >25 mm h^{-1}) associated with these convective storms are known to produce flash floods and debris flows even in unburned areas [*McCain and Shroba*, 1979].

[6] Geology in the near surface is primarily Boulder Creek granodiorite, with very limited exposures of quartz monzonite, quartz veins, and a geologic feature called the Iron Dike, consisting of diabase [*Gable*, 1980]. Soils are classified as the Allens Park member of the Fern Cliff-Allens Park-Rock outcrop complex, consisting of gravelly sandy loam that is a colluvium and/or residuum weathered from the predominant granodiorite [*Moreland and Moreland*, 1975]. Soils are described as frigid Lamellic and Typic Haplustalfa [*USDA*, 2010] (accessed 29 November 2010) and considered to be nonsaline and nonsodic [*Moreland and Moreland*, 1975]. Development of soil horizons has a strong aspect control, with relatively thin O horizons on north-facing slopes in contrast to thicker A horizons on south-facing slopes [*Birkeland et al.*, 2003].

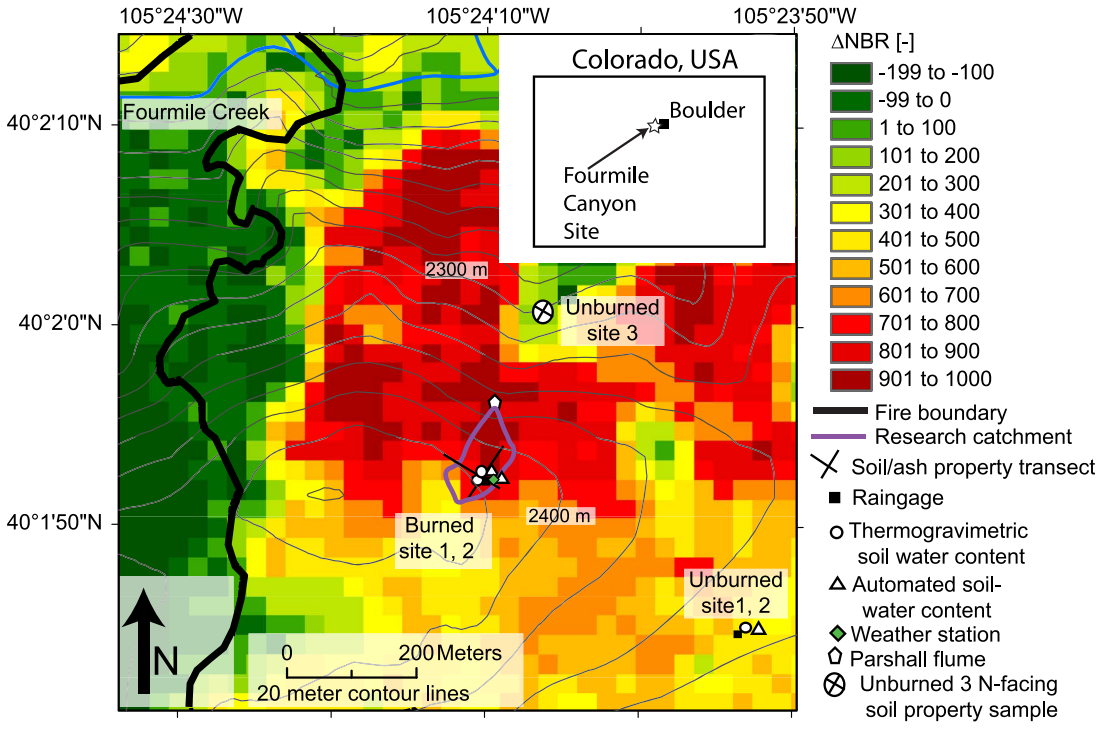

Figure 1. Map of the 2010 Fourmile Canyon Fire area in Colorado, USA near the city of Boulder showing the burned and unburned study site locations. The burn severity is quantified by Δ NBR, which is a remotely sensed metric [*Key and Benson*, 2005; *Keeley*, 2009]. Dark green is unburned and dark red is high burn severity. Pixel averaging makes the unburned site, which is a small pocket of unburned area near the fire edge, appear as low burn severity. The fire boundary shown as a solid black line in the inset is only a portion of the 6240 ha Fourmile Creek basin. Basemap by Sheila Murphy, USGS. Burn severity data from the USGS EROS Center.

[7] The site is in a Montane ecosystem [after *Marr*, 1961] with a forest classification of Foothill *Pseudotsuga-Pinus ponderosa* forest [*Peet*, 1981], and vegetation is controlled by aspect. Before the fire, trees were mostly ponderosa pine (*Pinus pondersosa*) interspersed with Rocky Mountain Juniper (*Juniperus scopulorum*) on south-facing slopes and aspen (*Populus tremuloides*), Rocky Mountain Douglas fir (*Pseudotsuga menziesii* subspecies *glauca*), and Limber pine (*Pinus flexilis*) on north-facing slopes [*FEST*, 2010]. Understory vegetation consisted of common juniper (*Juniperus communis*), mountain ninebark (*Physocarpus monogynus*), Kinnikinnick (*Arctostaphylos uva-ursi*), spike fescue (*Leucopoa kingii*), mountain muhly (*Muhlenbergia montana*), Arizona fescue (*Festuca arizonica*), and sedge (*Cyperaceae* spp.) [*Moreland and Moreland*, 1975; *Peet*, 1981].

2.2. The Fourmile Canyon Fire

[8] The Fourmile Canyon Fire began on 6 Sep. 2010 and was contained on 13 Sep. 2010 [*FEST*, 2010]. Conditions were dry before the wildfire; for example, from 1 August 2010 until the fire was contained, the nearby city of Boulder received only 32.5 mm of precipitation, which is approximately half of the average for August. The Front Range Foothills, in general, received 25% to 50% of normal precipitation, depending on the location [*Snider*, 2010]. High winds, coupled with relative humidities as low as 5% [*Snider*, 2010], drove an intense fire that changed directions multiple times. It spread quickly resulting in a patchy burn pattern of low, moderate, and high burn severities (Figure 1) spread over approximately 2500 ha [*FEST*, 2010]. The burn severity map represents an index calculated from data collected by the Landsat satellite platform to represent the change in land surface characteristics in response to fire [see *Keeley*, 2009]. In terms of personal property damage, it was the costliest fire in Colorado history, with 166 homes destroyed resulting in an estimated $217 million in losses; approximately 300 intact homes [*FEST*, 2010] lie within the burned area perimeter, increasing the potential for additional damage from postfire runoff and flooding.

2.3. Hillslope Field Sites

[9] To investigate the effects of wildfire on near-surface hydrologic states and processes, we selected a field site with a high burn severity on a north-facing hillslope in the Fourmile Creek drainage and a companion unburned site in the Bummers Gulch drainage on a south-facing hillslope (Figure 1). Additional unburned soil samples and in-situ hydraulic property measurements were collected from a north-facing hillslope site (Figure 1). The burned field site was a first-order catchment where the geology and soils could be assumed to be approximately the same. The boundaries of the drainage area were measured with a GPS unit (horizontal accuracy ~4–6 m depending on location) and the drainage area is approximately 7800 m^2 with local slopes ranging from 15° to 22° (mean of 17.5°) in the upper portion of the catchment and ranging from 20° to 28° (mean of 24°) in the lower portion of the catchment. The south-facing unburned sites had a local slope of 7° to 14° (mean of 11°). We use "burned" soils to mean that some organic matter may have been combusted, while the mineral component of soil was only heated.

3. Methods of Postwildfire Measurements

[10] On 14 Sep. 2010, one day after full wildfire containment (eight days after the wildfire started), we began to install instruments and collect soil samples from the burned and unburned field sites (Figure 1). Monitoring continued until 8 November 2010 when all precipitation began falling as snow and within a week the soil temperature at 5 cm depth was below 0°C.

3.1. Soil Physical and Hydraulic Properties

3.1.1. Physical Properties

[11] Ash thickness and soil particle size distribution were measured within the burned area along two perpendicular (100 m long) transects on 14 October 2010. One 100 m transect followed a contour in the upper part of the burned catchment and the second 100 m transect approximated a fall line with its midpoint collocated with the midpoint of the first transect. Samples were collected outward from this common midpoint at intervals of 0.1 m for five samples, at intervals of 1 m for five samples, and at intervals of 10 m for five samples. This nested sampling strategy produced three different scales (0.1, 1.0, and 10 m), with 21, 20, and 20 samples, respectively. To collect ash samples, a small (about 0.05 m) trench was cut into the soil, the ash thickness on top of the soil was measured and then removed by inserting a thin sharpened trowel at the ash-soil interface. A soil core (4.7 cm diameter, 3 cm long) was collected for particle size analysis and for selected organic content analysis. Samples were taken back to the laboratory and dried at 105°C for 24 h and then dry sieved at standard class sizes using standard procedures [see *Guy*, 1969].

[12] Soil cores for thermogravimetric soil water content analyses were also collected from the burned and unburned sites and used to measure soil properties including bulk density, particle-size distribution, and organic content. Organic content was measured for one set of samples collected on 27 October 2010 from two sites in the north-facing burned area (burned 1 and burned 2 sites), and from two sites in the unburned area (south-facing unburned 2 and north-facing unburned 3 shown in Figure 1). Samples from the north-facing sites were collected at 0–1.6 cm and from 1.6–3.0 cm below the surface. Samples were dried at 105°C for 24 h and the organic content was measured as the percent loss on ignition (LOI) after heating at 550°C for 4 h [*Heiri et al.*, 2001].

3.1.2. Hydraulic Properties

[13] Soil water retention curves for the burned and unburned soil and ash were measured in order to convert soil water content to matric potential. Intact cores (one core from each site) and ash (repacked to the field-measured bulk density) were analyzed in the laboratory. Soil water retention data were measured using the hanging column method [*Dane and Hopmans*, 2002a], pressure plate [*Dane and Hopmans*, 2002b], dewpoint potentiometer [*Gee et al.*, 1992], and a relative-humidity-controlled chamber [*Nimmo and Winfield*, 2002]. Saturated hydraulic conductivity (K_{sat}) was estimated using the constant head permeameter method [*Reynolds and Elrick*, 2002]. *Van Genuchten* [1980] parameters were estimated using RETC [*van Genuchten et al.*, 1991]. The soil water retention data also provide estimates of saturated soil water contents. Soil water retention in the

dry range (i.e., $\Theta \leq 0.05$ cm^3 cm^{-3}) was also estimated using the *Rossi and Nimmo* [1994] relation. An average of the *Rossi and Nimmo* [1994] proportionality constant α_{RN} was estimated for each data set for the dry range using a least-squares best fit to the measured soil water retention data. The value of the matric potential at zero soil water content ψ_D was estimated by graphical interpolation through the measured data to the intercept. The ψ_D value of -1×10^7 cm was consistent for ash, burned soil, and unburned soil and is a typical value [*Rossi and Nimmo*, 1994].

[14] Falling head infiltration ring tests with a 15 cm diameter ring [*Nimmo et al.*, 2009] were used to estimate field-saturated hydraulic conductivity (K_{fs}) ($L\ T^{-1}$) for burned soils with and without ash cover and unburned soils. Initial ponded head values of 5–6 cm were used, which exceeds ash storage capacity and were likely sufficient to overcome any increased water entry pressures cause by water repellency. Sorptivity and K_{fs} of burned and unburned soils were also measured using a small tension infiltrometer (4.4 cm diameter Minidisk, Decagon Devices Inc.) during the period from 8 October to 8 November 2010. The ash or litter layer was removed before starting the measurement. To ensure one-dimensional flow, a 4.4 cm diameter coring ring was inserted flush with the top of the soil (3 cm into the soil) and the tension infiltrometer with a 4.4 cm diameter was placed on the soil within the ring. A tension of -1.0 cm was used for all measurements. If no water infiltrated after 15–20 min the measurement was stopped. A second-order polynomial curve was fit to the cumulative infiltration volume versus square root of time, and sorptivity, S ($L\ T^{-0.5}$) and K_{fs} were computed using a one-dimensional solution for cumulative infiltration [*Vandervaere et al.*, 2000; *Moody et al.*, 2009] with the integral shape parameter β equal to 0.6 [*Haverkamp et al.*, 1994]. In this work we are assuming that K_{sat} and K_{fs} are isotropic and thus we refer to the magnitude of the value.

3.2. Hydrologic States

3.2.1. Soil Water Content

[15] Shallow soil cores from the near surface (0–3 cm) were collected at one to two day intervals at two locations in the burned area (burned 1 and burned 2) and one location in the unburned area (unburned 1). The thermogravimetric samples were collected within a several square meter area at a given site over the entire period of measurement. Soil water content Θ was estimated for these samples using thermogravimetric methods [*Topp and Ferré*, 2002]. Ash sampling for water content began on 25 Sep. 2010 at the burned 2 sampling site in the burned area. The reported thermogravimetric measurements are the mean of four replicate samples ($\sim$60 g each), collected at the sites. Samples were weighed to 0.001 g with an estimated error of $\pm$0.005 g or <0.01%. Bulk density was computed using dry weights and the core volume for each sample for the conversion from gravimetric to volumetric soil water content.

[16] Subsurface sensors were installed in the burned and unburned areas (Figure 1) to estimate soil water content, soil temperature, and bulk electrical conductivity (Decagon Devices 5TE). Sensors were installed by digging an access trench and inserting the sensor into undisturbed soil and carefully backfilling. Data were logged at 1 min temporal resolution from sensors installed at the unburned 2 site at 5, 10, and 15 cm depths (unburned A2) and from sensors installed at two sites in the burned area, burned A1 (5, 10, 15 cm depth) and burned A2 (5 and 10 cm depth). Sensors were calibrated in the laboratory using soil from each specific site and the technique recommended by *Cobos and Chambers* [2010].

3.2.2. Matric Potential

[17] Soil temperature and soil-gas relative humidity sensors (Onset U12–011) were installed in the subsurface in the burned 1 site (3 and 6 cm deep) and in the unburned 2 site (5 cm deep) to estimate matric potential using the Kelvin equation [*Koorevaar et al.*, 1983]. The sensors were installed using a small access trench to excavate a shallow section of soil, which was then backfilled around the sensor. The Kelvin equation method was applicable because of the very low matric potential values after the fire. We have assumed equilibrium between the soil-water and soil-gas and negligible osmotic potentials (i.e., nonsaline conditions). Data from the temperature and relative humidity sensors in the burned and unburned areas are not shown after the rainfall on 12 October 2010 because the relative humidity values rise above 90%, where the instrument accuracy and the large change in matric potential for a small change in relative humidity cause these estimates to have large errors. An additional estimate of matric potential in the subsurface was provided by converting the soil water content measurements (from the Decagon 5TE probes) to matric potential using the *van Genuchten* [1980] relation (when $\Theta > 0.05$ cm^3 cm^{-3}) and *Rossi-Nimmo* [1994] relation (when $\Theta \leq 0.05$ cm^3 cm^{-3}).

3.3. Rainfall and Runoff Measurements

[18] Burned and unburned areas were instrumented with a manual (i.e., visual) raingauge to record total rainfall between field visits and an automated tipping-bucket raingauge (0.254 mm per tip) for continuous monitoring. Cumulative precipitation from the automated raingauge was digitized using piecewise linear interpolation to a regular interval from which 5 min rainfall intensity was computed. Backward extrapolation from the first three tips was used to estimate the starting time of rainfall. A modified 3 in. Parshall flume was installed along the channel in the burned catchment to measure surface runoff discharge. Water depth in the flume was monitored at 10 s temporal resolution with an ultrasonic sensor (M5000, Massa Products Corp, Hingham, Mass.), which has an accuracy of $\pm$0.1 cm and a resolution of 0.025 cm over a range from 0 to 33 cm. Water depths or stages were converted to water discharge using on-site calibrations of stage and discharge. The resulting stage-discharge relation was nearly the same as the theoretical rating curve for a 3 in. Parshall flume published by *Kilpatrick and Schneider* [1983]. Flumes were cleaned 2–3 times per week to remove any debris or sediment deposited by previous runoff.

4. Results

4.1. Soil Physical and Hydraulic Properties

4.1.1. Physical Properties

[19] Ash thickness varied by spatial scale, whereas soil particle size distribution did not. The ash layer consisted of various forms of burned organic material, an average of 5.4% uncombusted organic material, and mineral soil

particles in the silt and fine sand class. Ash thicknesses represent some redistribution caused by strong gusty winds (gust to 30–60 km h^{-1}) on 20 and 23 Sep. 2010. The mean ash thickness along the two transects was 1.8 cm and had the least spatial variability at the 0.1 m scale (Table 1). Ash thickness was more variable at the 1 and 10 m scale. Particle size analysis of the mineral soil at the burned site expressed as percent gravel, sand, and fines (silt and clay) was essentially the same for all scales. The upper 3 cm of the burned soil was coarse grained and the mean of all 61 samples was 19% gravel (2–32 mm), 67% sand (0.063–2 mm), and 15% silt and clay (<0.063 mm). The burned soil had some large organic material composed of litter and in some locations substantial amounts of duff that were not fully combusted during the wildfire. The mass of this organic material compared to the mass of the mineral soil averaged about 6%, but there was a large degree of variability with a range from 0% to 41% and coefficient of variation of 1.5.

[20] Variability of ash thickness within the small scale of the burned 2 thermogravimetric site was less than the catchment scale variability (Table 1), with a σ of 0.67 cm. Mean ash thickness at the burned 2 thermogravimetric site was 1.8 cm, which was the same as the catchment mean (Table 1), suggesting that the burned 2 site was reasonably representative of catchment characteristics with respect to hydrological impacts of ash cover.

[21] A substantial amount of organic matter remained in the burned soils and in the ash, based on the LOI analysis from the 27 October 2010 sampling (Table 2). For the burned north-facing sites about 50% of the organic matter present before the fire remained in the near surface layer (0–1.6 cm, Table 2) and about 80% remained in the lower layer (1.6–3.0 cm) compared to the unburned north-facing site. The standard deviation (σ) and coefficient of variation (CV) in LOI (Table 2) show greater variability in organic content between soil samples at the unburned north-facing site compared to the two burned sites.

4.1.2. Soil-Hydraulic Properties

[22] There were major differences in the measured K_{sat} and K_{fs} values between the ponded head methods and the tension infiltrometer. The laboratory permeameter measurements and the falling-head ring infiltrometer measurements showed similar trends and magnitudes, with values for burned soils greater than unburned soils and magnitudes in 10 s of cm h^{-1} (Table 3). There was considerable spatial variability in K_{fs} in burned soils observed in the ponded head infiltration ring measurements, for example the K_{fs} values in the burned area ranged from 8 to 88 cm h^{-1} and for the unburned area from 21 to 33 cm h^{-1}. The variability in K_{fs} made it difficult to generalize about the differences in between burned and unburned soils based solely on the ring infiltrometer measurements. The tension infiltrometer measurements, which were applied at −1 cm tension rather than a ponded head, showed very different results and indicate that burned soils had considerably lower K_{fs} values than unburned soils (Table 3); note that ash had been removed prior to the burned soil measurements. This contrast in K_{fs} between burned and unburned soils was even starker when considering that at the north-facing burned sites K_{fs} was essentially zero because 9 out of the 12 tension infiltrometer measurements were stopped after 15–20 min because no water had infiltrated into the burned soil. Initial soil water content for these measurements ranged from 0.019 to 0.10 cm^3 cm^{-3} which was consistent with the dry initial conditions in near-surface soil that preceded runoff events.

Table 2. Loss on Ignition (LOI) [*Heiri et al.*, 2001] Results From the 27 October 2010 Sampling[a]

Site	Depth (cm)	LOI (%)	σ[b] (%)	CV[c] (–)
Burned 1 Soil[d]	0–3	3.3	0.4	0.12
Burned 2 Ash[d]		5.4	2.1	0.39
Burned 2 Soil[d]	0–1.6	6.1	1.6	0.26
	1.6–3	3.5	0.6	0.17
Unburned 2 Soil[e]	0–3	8.1	1.7	0.21
Unburned 3 Soil[d]	0–1.6	11	4.4	0.40
	1.6–3	4.4	2.0	0.45

[a]Locations shown in Figure 1.
[b]SD.
[c]Coefficient of variation.
[d]North-facing aspect.
[e]South-facing aspect.

4.2. Hydrologic States

4.2.1. Thermogravimetric Soil Water Content

[23] Time series of thermogravimetric soil water content measurements highlight the contrast in hydrologic states, before and after precipitation (Figure 2a), in near-surface soils and in ash immediately following wildfire (Figure 2b). Dry conditions persisted in burned soils and ash for weeks

Table 1. Ash Thickness and Soil Particle Size Distribution From the Two Transects Across the 1 ha Burned Field Site (Figure 1)

	Ash Thickness					Soil Particle Size Distribution			
Scale[a] (m)	Mean (cm)	Maximum (cm)	Minimum (cm)	σ[b] (cm)	CV[c] (–)	Gravel[d] (%)	Sand[e] (%)	Silt and Clay[f] (%)	Large Organics[g] (%)
0.1	1.8	4.0	0.5	1.1	0.6	17	68	15	5
1	2.0	8.0	0.1	2.1	1.0	19	66	15	6
10	1.4	4.5	0.1	1.2	0.9	20	65	15	10
All	1.8	8.0	0.1	1.6	0.9	19	67	15	6

[a]Distance between samples.
[b]SD.
[c]Coefficient of variation.
[d]2–32 mm.
[e]0.063–2 mm.
[f]<0.063 mm.
[g]Large organics are pieces of vegetative debris >2 mm.

Table 3. Mean Saturated Hydraulic Conductivity (K_{sat}), Field Saturated Hydraulic Conductivity (K_{fs}), and Sorptivity (S) Measured Using Three Different Techniques in Burned and Unburned Soils[a]

Soil Sample	K_{sat}[b] (cm h^{-1})	N[c]	K_{fs}[d] (cm h^{-1})	N	K_{fs}[e] (cm h^{-1})	S[3] (cm s$^{-0.5}$)	N
Ash[f]	0.86	(1)	–	–	–		–
Burned 2 soil[f,g]	27.4	(1)	41.1 ± 35.6	(5)	1.0 ± 2.8	0.00041 ± 0.0023	(12)
Unburned 2 soil[h]	12.4	(1)	26.8 ± 8.8	(2)	8.2 ± 4.7	0.019 ± 0.017	(4)
Unburned 3 soil[g]	–	–	–		72.0 ± 72.0	~0	(2)

[a]Variability is reported ±1 SD. Locations of samples are shown in Figure 1.
[b]Measured using a constant head permeameter in a laboratory [*Reynolds and Elrick*, 2002], only one sample core per site was taken so no σ is reported.
[c]N is number of measurements.
[d]Measured using a 15 cm diameter falling head infiltration ring [*Nimmo et al.*, 2009].
[e]Measured using a tension infiltrometer [*Moody et al.*, 2009].
[f]Ash was removed prior to measurements on burned soil.
[g]North-facing aspect.
[h]South-facing aspect.

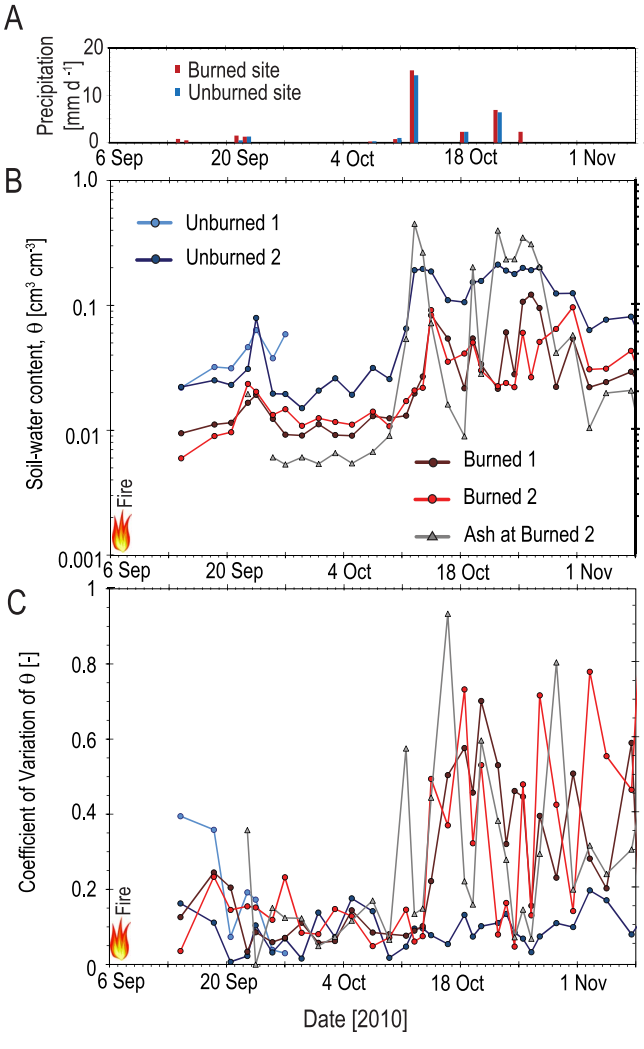

Figure 2. Time series of thermogravimetric soil water content θ representing the average from 0 to 3 cm depth for unburned soil, burned soil, and ash. (a) Time series of precipitation in the burned and unburned areas. (b) Base-10 logarithmic soil water content scale to show differences between burned and unburned soils at very low soil water contents. (c) Coefficient of variation (CV) of the soil water content time series shown in (b).

after the wildfire, relative to unburned soils (Figure 2b and Table 4). There was a substantial difference in the soil water content response of the ash, burned, and unburned soil to precipitation inputs (Figure 2b). Ash responded rapidly to rainfall, even from small storms, for example the 2.3 mm (18 October 2010) and 1.3 mm (25 October 2010) and also lost water rapidly (via drainage or evaporation) after the larger storms of 15.2 mm (12 October 2010, rain and snow) and 6.5 mm (22 October 2010). Ash also showed large increases in water content with precipitation inputs (Table 4). In contrast, the burned soil showed a delayed response to precipitation (Table 4 and Figure 2b), possibly because of the "buffering" effect of the ash layer on top of the burned soil. For example, the burned soil had a multiple-day lag before soil water content increased after the 15.2 mm (12 October 2010) and 6.5 mm (22 October 2010) precipitation inputs. Unburned soil had rapid responses in water content to precipitation inputs and was intermediate in terms of the magnitude of the change in soil water content between the ash and the burned soil. Burned soil drained relatively rapidly, like the ash, after the same two largest storms (Figure 2b).

[24] The variability in hydrologic states such as soil water content at small (<10 cm) scales was profoundly changed after the first substantial rainfall. This is illustrated by the time series of the coefficient of variation of soil water content for each site (i.e., the variability between the four replicate samples) shown in Figure 2c. For the period from wildfire containment until the 15.2 mm storm on 12 October 2010, the coefficient of variation in soil water content was similar for the burned/ash sites and for the

Table 4. Volumetric Soil-Water Contents From Thermogravimetric Samples

Time Period (2010)	Soil-Water Content			
	Burned 1 (cm^3 cm^{-3})	Burned 2 (cm^3 cm^{-3})	Ash (cm^3 cm^{-3})	Unburned 2 (cm^3 cm^{-3})
14 Sep. to 11 Oct.[a]	0.019	0.013	0.012	0.030
11 Oct. (prestorm)	0.013	0.017	0.054	0.065
12 Oct. (poststorm)	0.020	0.021	0.451	0.190
20 Oct. (prestorm)	0.034	0.030	0.028	0.157
22 Oct. (poststorm)	0.021	0.024	0.40	0.212

[a]Mean during this period.

unburned site. After the rainfall on 12 October 2010, soil water content variability in the two burned soils and in the ash increased substantially (Figure 2c). This increased small-scale variability in soil water content persisted throughout the period of measurement, spiking again in response to the 22 October 2010 storm. In contrast, the unburned soil water content variability remained essentially the same throughout the measurement period, irrespective of rainfall inputs.

4.2.2. Automated Soil Water Content

[25] The automated 1 min records of soil water content showed the same substantial differences in unsaturated zone response between the unburned site and burned sites (Figure 3b) as observed for the thermogravimetric measurements. However, there was almost no change in soil water content deeper in the soil (Figure 3b) from the small magnitude, initial September storms (0.3–1.5 mm d^{-1}). The period between these initial small (~1 mm) storms until the 15.2 mm storm on 12 October 2010 illustrates the difference between the burned and unburned soil water contents at depth; the unburned soils were wetter than the burned soils at all depths (Table 5 and Figure 3b).

[26] The difference in the response in the burned versus unburned soil to larger storms is evident for the 15.2 mm event on 12 October 2010 (Figure 3b, Table 5), which started as rain (total of 8.6 mm) but ended as snow. Increases in soil water content at 5 cm depth at the burned sites ranged from 0.051 to 0.076 cm^3 cm^{-3}, while increases at 5 cm depth at the unburned site were 0.350 cm^3 cm^{-3} (Table 5). In response to the 22 October 2010 storm the burned sensors at 5 cm depth only increased by 0.012 to 0.014 cm^3 cm^{-3}, while the unburned soil water content sensor at 5 cm depth increased by 0.196 cm^3 cm^{-3} (Figure 3b, Table 5). Peak water contents in the unburned soils were larger in Figure 3b relative to Figure 2b because the short-lived peaks are better resolved by the 1 min sampling than by the less frequent thermogravimetric measurements.

4.2.3. Matric Potentials

[27] Matric potential data also showed that dry conditions prevailed in the burned area until the first substantial rainfall on 12 October 2010 (Figure 3c). Matric potential (calculated by the method of converting the soil water content using the retention curves, see section 3) indicated that an order of magnitude difference in matric potentials at 5 cm depth was present immediately after the wildfire (drier in the burned area than the unburned area) (Figure 3c). The difference in matric potential (calculated from relative humidity and the Kelvin equation) between the burned and unburned soils was less but still drier in the burned area. The mean values at 5 cm depth based on both methods were similar for each site before the 12 October 2010 storm (Figure 3c). Matric potentials at greater depths in the soil profile (10 and 15 cm) did not show the substantial differences that were observed at 5 cm during this period (Figure 3c). The matric potential response to the storms on 12 and 22 October 2010 mirrors the response in the automated water content record from which it was derived. Change in matric potential in the unburned area was extremely rapid and ephemeral while the matric potential response at the burned site was of smaller magnitude and happened over a longer period of time (Figure 3c). Differences in matric potential response between the burned and unburned soils

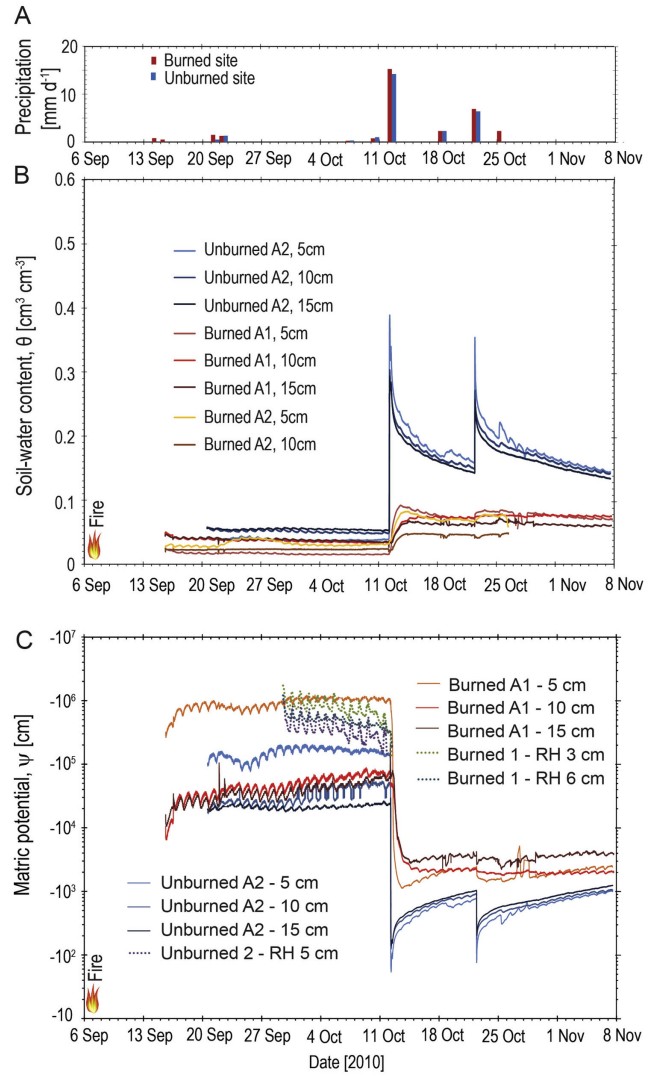

Figure 3. Automated measurements at 1 min temporal resolution of soil water content θ and matric potential ψ. The automated burned A1 and burned A2 sites were not the same location as the thermogravimetric burned 1 and burned 2 sites while the unburned A2 site was the same location as the thermogravimetric unburned site 2. (a) Time series of precipitation in the burned and unburned areas. (b) Soil water content. (c) Matric potential was calculated from relative humidity measurements using the Kelvin equation and by converting the soil water content data using the *van Genuchten* [1980] relations when $\theta > 0.05$ cm^3 cm^{-3} and the *Rossi and Nimmo* [1994] relations when $\theta \leq 0.05$ cm^3 cm^{-3}.

indicates that much less water infiltrated into the burned soil, compared to the unburned soil, consistent with the soil water content results shown in Figures 2b and 3b.

4.3. Runoff

[28] Two storms on 12 and 22 October 2010 produced runoff about one month following the wildfire. After both storms sediment was found in the flume, which we assumed was deposited during the falling limb of the hydrograph (see stippled area in Figures 4b and 4e). When the flume was cleaned out after the storm on 12 October 2010, the

Table 5. Volumetric Soil-Water Contents From Automated, 1 min Sensors Installed in Vertical Profiles

	Burned A1			Burned A2		Unburned A2		
Time Period (2010)	5 cm (cm^3 cm^{-3})	10 cm (cm^3 cm^{-3})	15 cm (cm^3 cm^{-3})	5 cm (cm^3 cm^{-3})	10 cm (cm^3 cm^{-3})	5 cm (cm^3 cm^{-3})	10 cm (cm^3 cm^{-3})	15 cm (cm^3 cm^{-3})
15 Sep. to 11 Oct.[a]	0.017	0.037	0.038	0.032	0.023	0.038	0.051	0.055
12 Oct. (prestorm)[b]	0.016	0.033	0.034	0.032	0.024	0.039	0.048	0.053
12 Oct. (poststorm)[c]	0.092	0.067	0.068	0.083	0.048	0.389	0.303	0.293
22 Oct. (prestorm)[b]	0.071	0.072	0.061	0.066	0.046	0.158	0.149	0.142
22 Oct. (poststorm)[c]	0.078	0.085	0.073	0.078	0.049	0.354	0.272	0.257

[a]Mean during this period.
[b]Value at onset of rainfall.
[c]Peak values following storm.

sediment was 4 cm thick. This depth corresponded to the depth measured by the ultrasonic sensor. Discharge during the remainder of the falling limb was estimated visually (dashed line in Figures 4b and 4e). For the 12 October 2010 storm, the rainfall was intermittent, but lasted about 140 min before runoff was initiated (Figures 4a and 4b). Rainfall statistics for the entire storm were a mean intensity of 2.7 mm h^{-1}, maximum intensity of 5.5 mm h^{-1}, and total rainfall of 8.6 mm (Figure 4a). Snowfall began at 10:00 A.M., lasting until 11:50 A.M. MDT, which did not generate runoff. In contrast to the 12 October 2010 storm, the 22 October 2010 storm was shorter and had higher rainfall intensity and runoff began sooner, after approximately 32 min of rainfall (Figure 4e). Rainfall statistics for this second storm were a mean rainfall intensity of 5.4 mm h^{-1}, maximum intensity of 10.7 mm h^{-1}, and a total rainfall of 6.5 mm (Figure 4d). Thresholds of runoff generation in terms of rainfall depth were 5.5 and 3.6 mm and the cumulative discharges were 0.97 and 1.32 m^3 for the 12 and 22 October 2010 storms, respectively. Despite large differences in the rainfall characteristics of the two storms, the peak discharges were similar, 1.20×10^{-3} m^3 s^{-1} (12 October

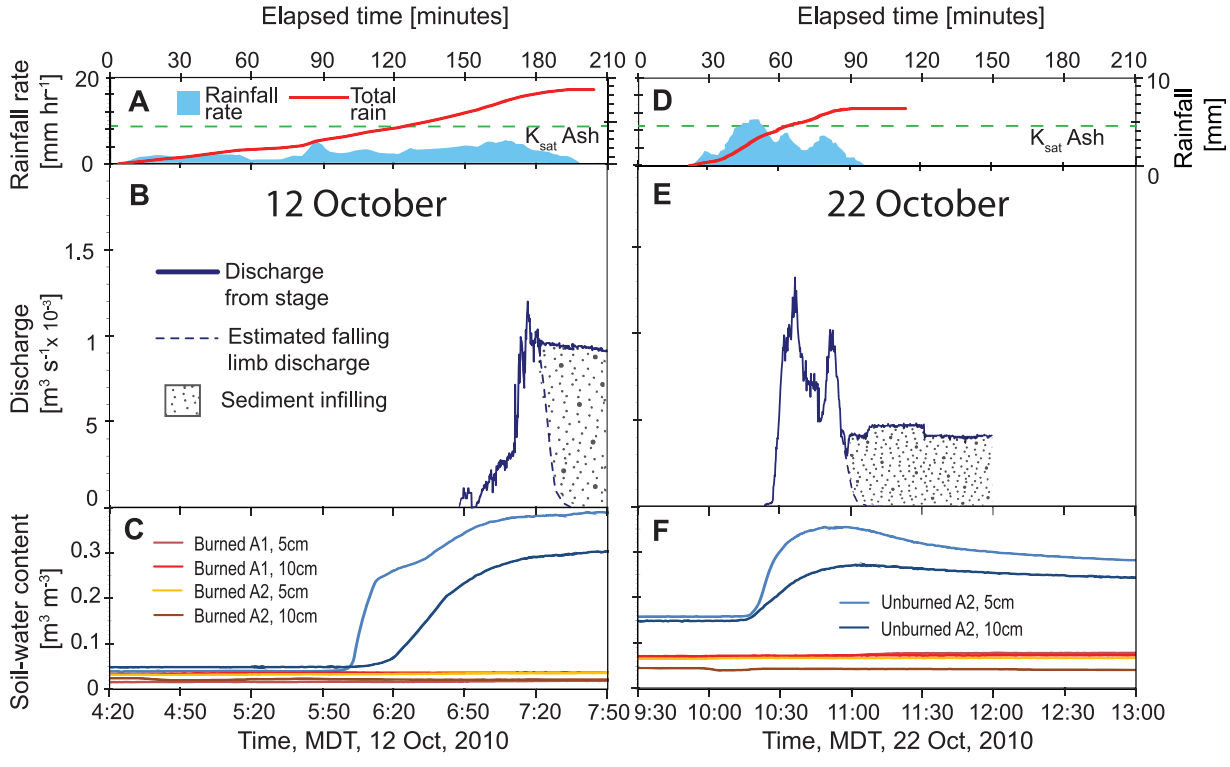

Figure 4. Time series of hydrologic data from the first two runoff-producing storms immediately after the wildfire. (a) Precipitation rate and total precipitation in the burned area computed from the tipping bucket raingauge, as 5 min data, for the 12 October 2010 storm. (b) Runoff hydrograph from the burned catchment during the 12 October 2010 storm. Sediment was deposited during the falling limb of the hydrograph producing a constant stage after the storm. The falling limb was visually estimated and the stippled area represents sedimentation. (c) Automated soil water content measurements in the burned and unburned sites during the 12 October 2010 storm. (d) Precipitation rate and total precipitation in the burned area computed from the tipping bucket raingauge, as 5 min data, for the 22 October 2010 storm. (e) Runoff hydrograph from the burned catchment during the 22 October 2010 storm. (f) Automated soil water content measurements in the burned and unburned sites during the 22 October 2010 storm.

2010) and 1.41×10^{-3} m^3 s^{-1} (22 October 2010). Soil water contents did not change in burned soils during the time scales of either storm (Figures 4c and 4f), whereas the unburned soils showed rapid rises during both storms (Figures 4c and 4f). We did not measure runoff in the unburned soil, however, field observations in the unburned area did not indicate overland flow, compared to the obvious rill generation and downslope sediment deposition seen in the burned area.

5. Discussion

5.1. Physical and Hydraulic Properties

[29] A major effect of wildfire was to partially or completely remove the organic litter/duff layer and replace it with an ash layer of varying thickness. We observed 50% (0–1.6 cm depth) to 20% (1.6–3.0 cm depth) reductions of soil-organic content in north-facing burned soil relative to north-facing unburned soil (Table 2). These reductions are consistent with previous observations of soil organic content reduction after wildfire [e.g., *Certini*, 2005]. For example, *Kane et al.* [2007] found 43 to 77% of soil organic carbon was removed by wildfire. *García-Oliva et al.* [1999] showed 32% reductions in soil organic carbon. The reduction of soil-organic content following wildfire is important because it affects soil water retention [*Riley*, 1979; *Rawls et al.*, 2003] and soil water retention impacts the initial conditions prior to rainstorms, which in turn imposes controls on runoff generation.

[30] Mean ash thickness at the Fourmile Canyon site was 1.8 cm, but varied from 0.1 to 8 cm thick (Table 1). The mean ash thicknesses reported here are within the range of values from other wildfire sites. For example, *Zavala et al.* [2009] reported a mean plot-scale ash thickness of 4.1 cm. *Woods and Balfour* [2008] showed a plot-scale mean ash thickness of 1.9 cm with ranges in mean ash thickness across their six plots from 1.0 to 3.4 cm. Mean ash thickness values are commonly several cm [e.g., *Ulery et al.*, 1993; *Cerdà and Doerr*, 2008; *Cannon et al.*, 2001], but can be less than 1 cm [*Goforth et al.*, 2005]. The variability in ash thickness we observed is greater than other sites, for example *Woods and Balfour* [2008] reported plot-scale standard deviations of 1.0 cm or less. Ash thickness and ash soil water content determine the initial water storage capacity prior to rainfall, and thus, the time to ponding and rainfall depth threshold necessary for runoff generation.

[31] Wildfire substantially reduced K_{fs}, which was shown by the almost 2 orders of magnitude lower K_{fs} in burned north-facing soil compared to unburned north-facing soil (Table 3) and that 9 out of the 12 measurements on burned soils were impermeable at the time scale of rainstorms. This was verified by field observations made during the rain storm on 22 October 2010 when wet ash layers at two different locations were scraped aside and revealed soil that was "bone" dry under both locations. The substantial reductions in K_{fs} observed at the Fourmile Canyon site are consistent with observations at other burned sites. For example, *Nyman et al.* [2010] reported a sevenfold decrease in the in-situ values of K_{sat} in burned soils relative to unburned soils one month after fire containment. We believe that under the dry conditions present at the burned site reported here that these tension infiltrometer results, showing near-zero K_{fs} in the burned soil at slightly negative matric potential, are indicative of the "true" K_{fs}. Measurements of K_{fs} using a ponded head overwhelm the factors that drastically reduce hydraulic conductivity in burned soils. This also is in agreement with the conclusions of *Nyman et al.* [2010]. These results highlight the importance of in-situ measurements (versus laboratory analysis) and measurement conditions that are physically consistent with conditions during runoff generation (i.e., not ponded heads of several cm) for measuring K_{fs} for use in runoff generation analysis.

[32] There is an important distinction to be made between "static" (i.e., quasi time-invariant) properties like K_{fs} versus dynamic changes in infiltration capacity that can result from changes in the soil surface during rainstorms. For example, some studies have shown that surface soil crust formation [*Mills and Fey*, 2004] and ash clogging of near surface soil pores during a storm or with progressive storm cycles can decrease infiltration capacities [*Mallik*, 1984; *Onda et al.*, 2008] from immediate postwildfire capacities. However, crusting or surface seal formation was not an issue in our research site, which had a layer of ash to absorb raindrop impact. This was demonstrated by *Woods and Balfour* [2008] in a plot-scale runoff generation study, where a loose, deformable ash layer reduced raindrop impact, thus preventing surface seal formation. This suggests that in ash-covered catchments, such as the Fourmile Canyon site, that our measurements of K_{fs} are suitable for analyzing runoff generation processes without considering surface sealing, provided the ash layer is present.

5.2. Hydrologic States

[33] During the immediate period after the wildfire, the burned soils were drier than unburned soils (Figures 2b and 3b, Tables 4 and 5), and it is clear from the soil water content time series that the burned soils did not respond at all during the time scales of either storm (Figures 4c and 4f), indicating almost no infiltration into the soil. In contrast, the unburned soils showed rapid rises during both storms, suggesting high infiltration capacities (Figures 4c and 4f). The soil water content difference between burned and unburned soils became larger following the two storms on 12 and 22 October 2010 (Figures 2b and 3b, Tables 4 and 5), which indicates that less rainfall infiltrated into the burned soils than the unburned soils. These results are consistent with work at other burned sites, which consistently had lower soil water contents [*Campbell et al.*, 1977; *Moody et al.*, 2007], relative to unburned sites, because of decreased infiltration and increased evaporation. Observed matric potentials indicated about one order of magnitude difference prior to the 12 October 2010 storm, with smaller matric potentials in burned soils than in unburned soils. Similarly, *Soto et al.* [1993] instrumented plots with tensiometers and found that in the top 5 cm of soil, matric potentials in the burned plot were smaller than matric potentials in the unburned plot.

[34] The thermogravimetric soil water content measurements showed substantial small-scale (~5–10 cm) spatial variability within the ash and burned soil, however the exact cause of the variability is enigmatic. Other studies have also shown similar variability; for example, *Moody et al.* [2007] found that burned soils exhibit more spatial variability in soil water content than unburned soils at a different

wildfire site in the Colorado Front Range of the Rocky Mountains, USA. Centimeter-scale variability in hydraulic conductivity in burned soils, reported by *Nyman et al.* [2010], may be a contributing factor to the centimeter-scale variability in soil water content observed in our research site. We did not observe variations in particle-size distribution, which would indicate differences in soil water retention, at the centimeter scale sufficient to cause such large variations in soil water content (Table 1). The variability in soil water content in the burned soils may also be attributable to variations in organic content, although Table 2 shows that organic content variability was actually larger in the unburned soils. It is likely that the large soil water content variability in the burned soils is a complex combination of factors relating hydrologic states to hydraulic properties like hydraulic conductivity and soil water retention, influenced by spatial variations in ash thickness and organic content.

[35] The differences in hydrologic states (i.e., soil water content and matric potential) and spatial variability in these states between burned and unburned soils may be important for runoff generation processes because it may affect the connectivity pattern of runoff producing soil patches. It is well known that runoff generation depends on initial conditions in unburned soils [e.g., *Zehe and Blöschl*, 2004]. Given the role of soil water repellency in runoff generation in burned soils [e.g., *DeBano*, 2000; *Letey*, 2001] and the dependence of soil water repellency on hydrologic states (i.e., drier soils enhance repellency) [e.g., *Doerr and Thomas*, 2000; *Regalado and Ritter*, 2009], burned catchments may be particularly sensitive to the dry initial hydrologic conditions shown herein, but in the opposite trend of unburned catchments (where wet initial conditions are more conducive to runoff generation).

5.3. The Role of Ash in Controlling Runoff Generation

[36] Ash spatial variability and the spatial organization of that variability (i.e., connectivity) control how isolated contributing areas for runoff connect at the catchment scale, and thus impact runoff timing and amount. Ash had a much larger infiltration capacity than the nearly impermeable burned soil and a large saturated soil water content of 0.58 $cm^3\ cm^{-3}$ (based on laboratory measurements on intact cores), which facilitated storing large amounts of water for a given thickness. Ash-stored water drained over a period of 1–2 days into the underlying burned soil or evaporated back into the atmosphere (Figures 2b and 3b). The capability of the ash to act as a reservoir and slowly release water into burned soils with relatively low infiltration capacities can provide an important "buffering" of hydrologic response in recently burned areas, similar to the plot-scale findings by *Woods and Balfour* [2010]. Very few studies have shown the effects of ash on runoff generation at catchment scales [see *Campbell et al.*, 1977]. Our results indicate that ash delays and dampens the soil water content response of the soil. Our burned site is a sandy soil with gravel and stones, and thus corresponds to the situation highlighted by *Woods and Balfour* [2010] of a thick (i.e., ~2 cm or greater) ash layer that results in the reduction of runoff. The ash layer is, however, temporary and is reduced and eventually removed by aeolian and hydraulic erosion. When the ash layer decreases to some critical thickness, its role as buffer diminishes, and the remaining fines from ash can clog the coarse-textured soil, reducing infiltration capacity [e.g., *Onda et al.*, 2008; *Woods and Balfour*, 2008] and potentially causing increased runoff. Therefore, it may be advantageous to apply postwildfire hillslope treatments such as mulching immediately after a wildfire, before ash is removed, to retain the buffering role of ash in controlling runoff generation.

5.4. Runoff Generation Mechanisms and Sensitivity

[37] Discerning exactly how runoff is generated for the two very different October storms is complicated. The peak rainfall intensities during the 22 October 2010 storm were about twice as high as the 12 October 2010 storm, yet the peak discharges were nearly the same, as were the runoff durations and total discharge volumes. Automated soil water content sensors in the burned area (Figures 4c and 4f) did not indicate soil water contents remotely close to saturation (based on the core samples analyzed for soil water retention) during either storm, in either the unburned or burned soils, suggesting that any runoff was not generated by the saturation-excess mechanism at an interface deeper than 5 cm in the soil. Based on this evidence, saturation-excess runoff from an upward-propagating perched water table at an interface in the soil below 5 cm was not a runoff mechanism during either storm. Moreover, a distinct downward-propagating wetting front would be expected in the mineral soil from infiltration-excess runoff, but this was not seen arriving at the automated soil water content sensors in the burned area (Figures 3b, 4c, and 4d). The facts that a distinct ash layer of variable thickness covered most of the catchment (which others have observed to affect runoff, [*Woods and Balfour*, 2008, 2010]) and that there was essentially no change in the soil water content within the burned soil layer below the ash layer in response to the rainfall suggests that the ash layer played a critical role in controlling runoff generation during these two storms.

[38] One hypothesis is that the long duration, low intensity rainfall (Figure 4a) during the 12 October 2010 storm saturated the thin ash layer, thus generating saturation-excess runoff. The tension infiltrometer measurements of K_{fs} during this period showed that the burned soils were essentially impermeable, which is consistent with the formation of a perched water table at the ash-soil interface. If saturation-excess runoff is generated at the ash-soil interface, then total discharge volume divided by the total rainfall depth after runoff initiation provides an estimate of the average contributing area during the saturation-excess generation period, which is 310 m^2. This estimate assumes no water drained from the ash into the soil on the storm time scale, which was supported by the automated water content data (Figure 4c). The total catchment area is approximately 7800 m^2, so the contributing area for the 12 October 2010 storm was about 4% of the total catchment area. Additionally, rainfall intensities during the 12 October 2010 storm never exceeded the ash K_{sat} (Table 3, Figure 4a), so runoff should not be generated by the infiltration-excess mechanism at the ash surface.

[39] Runoff generation for during the 22 October 2010 storm was quite different than during the 12 October 2010 storm, which was consistent with differences in the storm rainfall characteristics. The observed cumulative rainfall threshold (3.6 mm) for runoff generation for the 22 October

2010 storm was smaller than for the 12 October 2010 storm (5.5 mm). However, the maximum rainfall intensity was about twice as great for the 22 October 2010 (10.7 mm h^{-1}) than for the 12 October 2010 (5.5 mm h^{-1}) storm. Our field observations documented that some runoff during the 22 October 2010 storm was generated from a rocky area (~1300 m^2) at the eastern edge of the catchment with patches of the ash between the rocks. Before both storms, the initial conditions of soil water content in the ash were relatively dry (Table 4) so that the available water storage in the ash layer was nearly the same for both storms, which assumes the same ash saturated soil water content, 0.58 cm^3 cm^{-3}, and a threshold mean ash thickness of 1.0 cm corresponding to the thickness required to produce runoff at the threshold (5.5 mm) for the 12 October 2010 storm. Because the cumulative rainfall threshold for the 22 October 2010 storm was only 3.6 mm, saturation of the ash layer should not have happened, so that saturation-excess runoff does not adequately explain runoff generation during the 22 October 2010 storm, requiring an alternate hypothesis.

[40] The key to differentiating runoff generation between these two storms is the rainfall intensity compared to the ash K_{sat}. While it is the time-variable infiltration capacity (relative to rainfall intensity) that determines infiltration excess runoff, K_{sat} has been recommended as an approximation [e.g., *Rubin and Steinhardt*, 1962; *Freeze and Cherry*, 1979] and was used here in our analysis. The rainfall intensity during the 22 October 2010 storm exceeded the ash K_{sat} (8.6 mm h^{-1}, Table 3) for about 12 min from 10:10 to 10:22 A.M. (Figure 4d). Runoff in the flume started at 10:25 A.M. with peak discharge at 10:37 A.M. and second peak in discharge took place at 10:51 A.M. MDT (Figure 4e). The relative timing of rainfall intensities exceeding the ash K_{sat} and discharge at the flume points strongly to infiltration-excess runoff generation at the ash surface. Total infiltration-excess rainfall during the 22 October 2010 storm was 0.25 mm, defining excess infiltration rainfall as the total amount in excess of the ash K_{sat} during time periods when rainfall intensity exceeds ash K_{sat}. Total discharge volume was 1.32 m^3, giving a contributing area of ~5300 m^2, which was 68% of the total catchment area. Assuming zero infiltration into the burned soil at the storm time scale, which was well supported by the soil water content measurements (Figures 2b, 3b, 4c, and 4f), the comparison of the runoff to rainfall amounts for the two storms suggests that the ash stored 99% of rainfall for the 12 October 2010 storm and 97% of rainfall for the 22 October 2010 storm.

[41] Recent efforts have recognized that runoff generation from burned areas may not be solely by the infiltration-excess mechanism and that the saturation-excess mechanism and subsurface stormflow may also be important [*Soto et al.*, 1993; *Onda et al.*, 2008]. As noted by *Woods and Balfour* [2010], if ash storage is exceeded and the ash becomes saturated and the underlying soil is less hydraulically conductive than the ash, then runoff at the ash-soil interface would be classified as saturation excess. Spatial variability in ash thickness may result in saturation-excess runoff generation in areas of thin ash followed by "runon" [after *Smith and Hebbert*, 1979] in areas of thicker ash. Rainfall depth thresholds for initiation of saturation-excess runoff may then depend on achieving catchment-scale connectivity between saturated patches of thin ash. Saturation-excess thresholds for ash-mantled systems could be considered analogous to hillslope systems governed by soil-bedrock interfaces, where the topography of the interface also dictates the threshold behavior (e.g., the "fill and spill" model of *Tromp-Van Meerveld and McDonnell* [2006a, 2006b]).

[42] It is challenging to capture these threshold runoff-generating behaviors with distributed measurements in burned areas in the presence of thinly (~1–2 cm) ash-mantled slopes, thus we rely upon deciphering emergent properties at the catchment scale (i.e., runoff hydrographs) to determine runoff-generation mechanisms. One drawback to this approach is the sensitivity of the conclusions to the site-characterization data. Using the 22 October 2010 storm as an example, with total observed runoff held constant, if the K_{sat} of the ash is decreased by 0.5 mm h^{-1} then the estimated contributing area is ~3700 m^2, a 30% reduction in contributing area. An increase of 0.5 mm h^{-1} in ash K_{sat} requires a contributing area that is 600 m^2 more than the entire catchment area of 7800 m^2. The peak rainfall intensity during the 22 October 2010 storm was 10.7 mm h^{-1}, so an increase in the measured ash K_{sat} of only 25% could result in no runoff at all. The double-peaked runoff during the 22 October 2010 storm (Figure 4e) suggests that rainfall intensity was greater than infiltration capacity for more than one time period. This indicates that ash K_{sat} was lower than the measured value and that infiltration capacity may have not yet asymptotically reached the K_{sat} value during the October 22 2010 storm. Sensitivity to ash thickness is also high, in the case of saturation-excess runoff generation. For the 12 October 2010 storm with dry initial conditions in the ash, an ash thickness of 1.0 cm corresponds to the 5.5 mm observed rainfall threshold. If the ash was a uniform thickness throughout the catchment, equal to the mean (1.8 cm), then the rainfall depth threshold for 12 October 2010, with the same initial ash soil water content (Table 4), would be 9.7 mm and runoff could not have been generated by the saturation-excess mechanism at the ash-soil interface. Runoff generation mechanisms at this field site clearly hinge on both ash thickness and rainfall intensities relative to ash K_{sat}. Based on the two storms we observed, both the saturation-excess and infiltration-excess mechanisms can operate in a burned catchment. Furthermore, these two disparate runoff generation mechanisms may transpire during the same storm at different times. Our results have important implications for hydrologic models based solely on a specific runoff generation mechanism or that assume static contributing areas between storms.

6. Conclusions

[43] This research focused on the controls on runoff generation immediately after wildfire when an ash layer is present. Our investigation included the effects of wildfire on the physical and hydraulic properties of soil, hydrologic states, and the implications of these wildfire impacts for runoff generation. Dry hydrologic states, shown by volumetric water content and matric potential measurements, persisted in soils for a month after the wildfire, until the first major rainfall. Unsaturated zone hydrologic response, based on soil water content and matric potential time series, was substantially reduced in magnitude and delayed in

burned soils, relative to unburned soils, indicating a large reduction in infiltration into soils in the burned area. Burned soils showed substantial small scale (~5–10 cm) spatial variability in soil water content in the top 3 cm of soil in response to rainfall while unburned soil did not. Near-zero infiltration capacities into burned soil at the storm time scale were demonstrated by tension infiltrometer measurements. Ash acts as an important hydrologic buffer, storing water readily at the storm time scale of minutes and releasing water slowly over a period of several days into burned soils and by evaporation into the atmosphere. The essentially impermeable burned soil caused the ash layer to control runoff from the first two substantial storms after the wildfire. The hydraulic properties of ash, combined with the ash thickness, were capable of preventing, delaying, or greatly reducing runoff from burned areas for the two moderate storms we observed. Ash storage during the two storms ranged from 97% to 99% of rainfall, which was critical for reducing runoff amounts. Runoff was produced predominantly by the saturation-excess mechanism at the ash-soil interface for the first storm and predominantly by the infiltration-excess mechanism at the ash surface for the second storm, highlighting the large spectrum of runoff-generation behaviors operating at a site over a period as brief as 10 days. Estimated contributing areas during the two storms were 4% (saturation-excess runoff) versus 68% (infiltration-excess runoff) of the total catchment area, and these contributing area estimates were highly sensitive to ash thickness and ash hydraulic conductivity. Our results suggest that hydrologic models that do not include ash-controlled hydrologic processes or assume static contributing areas, regardless of runoff generation mechanism, may not provide accurate estimates of peak rates or total amounts of runoff in the few months immediately after a wildfire.

[44] **Acknowledgments.** This manuscript benefitted from discussions with Brian Andraski, Rick Healy, Eve-Lyn Hinckley, Jason Kean, Richard Martin, Ben Mirus, Sheila Murphy, John Nimmo, Petter Nyman, Luis Oteiro, Kim Perkins, Dennis Staley, Dave Stannard, David Stonestrom, Jeff Writer, and three anonymous reviewers. Brian Ebel received support from the Mendenhall Postdoctoral Fellowship Program in the National Research Program of the U.S. Geological Survey. Any use of trade, firm, or product names is for descriptive purposes only and does not imply endorsement by the U.S. Government.

References

Birkeland, P. W., R. R. Shroba, S. F. Burns, A. B. Price, and P. J. Tonkin (2003), Integrating soils and geomorphology in mountains—An example from the Front Range of Colorado, *Geomorphology*, *55*, 329–344.

Campbell, R. E., P. F. Baker, P. F. Folliot, F. R. Larson, and C. C. Avery (1977), Wildfire effects on a ponderosa pine ecosystem: An Arizona case study, *USDA Forest Service Research Paper RM-191*, U.S. Department of Agriculture, U.S. Forest Service, Fort Collins, CO.

Cannon, S. H., E. R. Bigio, and E. Mine (2001), A process for fire-related debris flow initiation, Cerro Grande fire, New Mexico. *Hydrol. Processes*, *15*, 3011–3023, doi:10.1002/hyp.388.

Cerdà, A., and S. H. Doerr (2008), The effect of ash and needle cover on surface runoff and erosion in the immediate post-fire period, *Catena*, *74*, 256–263, doi:10.1016/j.catena.2008.03.010.

Certini, G. (2005), Effects of fire on properties of forest soils: A review, *Oecologia*, *143*, 1–10, doi:10.1007/s00442-004-1788-8.

Cobos, D. R., and C. Chambers (2010), *Calibrating ECH2O Soil Moisture Sensors*, Application Note, Decagon Devices, Pullman, WA, 7 pp.

Dane, J. H., and J. W. Hopmans (2002a), Hanging water column, in *Methods of Soil Analysis, Part 4–Physical methods, Soil Science Society of America Book Series No. 5*, edited by J. H. Dane and G. C. Topp, pp. 680–683, Soil Science Society of America, Madison, WI.

Dane, J. H., and J. W. Hopmans (2002b) Pressure plate extractor, in *Methods of Soil Analysis, Part 4–Physical Methods, Soil Science Society of America Book Series No. 5*, edited by J. H. Dane and G. C. Topp, pp. 688–690, Soil Science Society of America, Madison, WI.

DeBano, L. F. (2000), The role of fire and soil heating on water repellency in wildland environments: A review, *J. Hydrol.*, *231–232*, 195–206, doi:10.1016/S0022-1694(00)00194-3.

Doerr, S. H., and A. D. Thomas (2000), The role of soil moisture controlling water repellency: New evidence from forest soils in Portugal, *J. Hydrol.*, *231–232*, 131–147.

Douglas, M. W., R. A. Maddox, K. Howard, and S. Reyes (2004), The North American Monsoon, Reports to the Nation on our Changing Planet, 25 pp, [Available at: http://www.cpc.noaa.gov/products/outreach/Report-to-the-Nation-Monsoon_aug04.pdf], NOAA/National Weather Service, Tuscon, Ariz.

Emelko, M. B., U. Silins, K. D. Bladon, and M. Stone (2011), Implications of land disturbance on drinking water treatability in a changing climate: Demonstrating the need for "source water supply and protection" strategies, *Water Res.*, *45*, 461–472.

FEST (Fourmile Emergency Stabilization Team) (2010), Fourmile Emergency Stabilization Burned Area Report, Boulder County, CO, 14 pp.

Freeze, R. A., and J. A. Cherry (1979), *Groundwater*, 604 pp., Prentice-Hall, New York.

Gabet, E. J., and P. Sternberg (2008), The effects of vegetative ash on infiltration capacity, sediment transport and the generation of progressively bulked debris flows, *Geomorphology*, *101*, 666–673, doi:10.1016/j.geomorph.2008.03.005.

Gable, D. J. (1980), Geologic map of the Gold Hill quadrangle, Boulder County, Colorado, *Geologic Quadrangle Map GQ-1525*, scale 1:24,000, U.S. Geological Survey, Reston, VA.

García-Oliva, F., R. L. Sanford Jr., and E. Kelly (1999), Effects of slash-and-burn management on soil aggregate organic C and N in a tropical deciduous forest, *Geoderma*, *88*, 1–12.

Gee, G. W., M. D. Campbell, G. S. Campbell, and J. H. Campbell (1992), Rapid measurement of low soil water potentials using a water activity meter, *Soil Sci. Soc. Am.*, *56*, 1068–1070.

Goforth, B. R., R. C. Graham, K. R. Hubbert, W. Zanner, and R. A. Minnich (2005), Spatial distribution and properties of ash and thermally altered soils after high-severity forest fire, southern California, *Int. J. Wildland Fire*, *14*, 343–354.

Gresswell, R. E. (1999), Fire and aquatic ecosystems in forested biomes of North America, *Trans. Am. Fish. Soc.*, *128*, 193–221.

Guy, H. P. (1969), Laboratory theory and methods for sediment analysis, *U.S. Geological Survey Techniques of Water-Resources Investigations*, Book 5, Chap. C1, 58 pp., U.S. Geol. Surv., Arlington, VA.

Haverkamp, R., P. J. Ross, K. R. J. Smettem, and J. Y. Parlange (1994), Three-dimensional analysis of infiltration form the disc infiltrometer 2. Physically based infiltration equation, *Water Resour. Res.*, *30*, 2931–2935.

Heiri, O., A. F. Lotter, and G. Lemcke (2001), Loss on ignition as a method for estimating organic and carbonate content in sediments: Reproducibility and comparability of results, *J. Paleolimnol.*, *25*, 101–110.

Ice, G. G., D. G. Neary, and P. W. Adams (2004), Effects of wildfire on soils and watershed processes, *J. For.*, *102*, 16–20.

Kane, E. S., E. S. Kasischke, D. W. Valentine, M. R. Turetsky, and A. D. McGuire (2007), Topographic influences on wildfire consumption of soil organic carbon in interior Alaska: Implications for black carbon accumulation, *J. Geophys. Res.*, *112*, G03017, doi:10.1029/2007JG000458.

Keeley, J. E. (2009), Fire intensity, fire severity and burn severity: A brief review and suggested usage, *Int. J. Wildland Fire*, *18*, 116–126.

Key, C. H., and N. C. Benson (2005), Landscape assessment: Remote sensing of severity, the Normalized Burn Ratio, in *FIREMON: Fire Effects Monitoring and Inventory System*, edited by D. C. Lutes, *General Technical Report RMRSGTR-164-CD*, pp. LA1–LA51, USDA Forest Service, Rocky Mountain Research Station. Ogden, UT.

Kilpatrick, F. A., and V. R. Schneider (1983), Use of flumes in measuring discharge, *Techniques of Water-Resources Investigations of the United States Geological Survey*, Book 3, Chap. A14, 46 pp., U.S. Geol. Surv., Arlington, VA.

Kitzberger, T., P. M. Brown, E. K. Heyerdahl, T. W. Swetnam, and T. T. Veblen (2007), Contingent Pacific–Atlantic Ocean influence on multicentury wildfire synchrony over western North America, *Proc. Natl. Acad. Sci.*, *104*, 543–548.

Koorevaar, P., G. Menelik, and C. Dirksen (1983), *Elements of Soil Physics*, Developments in Soil Science, Elsevier, Amsterdam.

Letey, J. (2001), Causes and consequences of fire-induced water repellency, *Hydrol. Processes*, *15*, 2867–2875, doi:10.1002/hyp.378.

Mallik, A. U., C. H. Gimingham, and A. A. Rahman (1984), Ecological effects of heather burning, I. Water infiltration, moisture retention and porosity of surface soils, *J. Ecol.*, *72*, 767–776.

Marr, J. W. (1961), Ecosystems of the east slope of the Front Range in Colorado, *University of Colorado Studies, Series in Biology No. 8*, 134 pp., University of Colorado, Boulder, CO.

McCain, J. F. and R. R. Shroba (1979), Storm and flood of July 31–August 1, 1976, in the Big Thompson River and Cache la Poudre River basins, Larimer and Weld Counties, Colorado, *U.S. Geol. Surv. Prof. Pap.* 1115-A,B, 152 pp., U.S. Geol. Surv., Washington, D.C.

Mills, A. J., and M. V. Fey (2004), Frequent fires intensify soil crusting: Physicochemical feedback in the pedoderm of long-term burn experiments in South Africa, *Geoderma*, *121*, 45–64, doi:10.1016/j.geoderma.2003.10.004.

Moody, J. A., and D. A. Martin (2001a), Initial hydrologic and geomorphic response following a wildfire in the Colorado Front Range, *Earth Surf. Processes Landforms*, *26*, 1049–1070, doi:10.1002/esp.253.

Moody, J. A., and D. A. Martin (2001b), Post-fire, rainfall intensity-peak discharge relations for three mountainous watersheds in the western USA, *Hydrol. Processes*, *15*, 2981–2993, doi:10.1002/hyp.386.

Moody, J. A., D. A. Martin, T. M. Oakley, and P. D. Blanken (2007), Temporal and spatial variability of soil temperature and soil moisture after a wildfire, *U.S. Geological Survey Scientific Investigations Report 2007-5015*, 89 pp., U.S. Geol. Surv., Reston, VA.

Moody, J. A., D. A. Kinner, and X. Ubeda (2009), Linking hydraulic properties of fire affected soils to infiltration and water repellency, *J. Hydrol.*, *379*, 291–303, doi:10.1016/j.jhydrol.2009.10.015.

Moreland, D. C., and R. E. Moreland (1975), *Soil Survey of Boulder County Area, Colorado*, 91 pp., Natural Resources Conservation Service, United States Department of Agriculture, Washington, D.C.

Neary, D. G., C. C. Klopatek, L. F. DeBano, P. F. Folliott (1999), Fire effects on belowground sustainability: A review and synthesis, *For. Ecol. Manage.*, *122*, 51–71, doi:10.1016/S0378-1127(99)00032-8.

Nimmo, J. R., and K. A. Winfield (2002), Miscellaneous methods [water retention and storage], in *Methods of Soil Analysis, Part 4–Physical methods, Soil Science Society of America Book Series No. 5*, edited by J. H. Dane and G. C. Topp, pp. 710–714, Soil Science Society of America, Madison, WI.

Nimmo, J. R., K. M. Schmidt, K. S. Perkins, and J. D. Stock (2009), Rapid measurement of field-saturated hydraulic conductivity for areal characterization, *Vadose Zone J.*, *8*, 142–149, doi:10.2136/vzj2007.0159.

Nyman, P., G. Sheridan, and P. N. J. Lane (2010), Synergistic effects of water repellency and macropore flow on the hydraulic conductivity of a burned forest soil, south-east Australia, *Hydrol. Processes*, *24*, 2871–2887, doi:10.1002/hyp.7701.n.

Onda, Y., W. E. Dietrich, and F. Booker (2008), Evolution of overland flow after a severe forest fire, Point Reyes, California, *Catena*, *72*, 13–20, doi:10.1016/j.catena.2007.02.003.

Pechony, O., and D. T. Shindell (2010), Driving forces of global wildfires over the past millennium and the forthcoming century, *Proc. Natl. Acad. Sci.*, *107*, 19167–19170.

Peet, R. K. (1981), Forest vegetation of the Colorado Front Range, *Plant Ecol.*, *45*, 3–75, doi:10.1007/BF00240202.

Prosser I. P., and L. Williams (1998), The effect of wildfire on runoff and erosion in native Eucalyptus forest, *Hydrol. Processes*, *12*, 251–265.

Rawls, W. J., Y. A. Pachepsky, J. C. Ritchie, T. M. Sobeckic, and H. Bloodworth (2003), Effect of soil organic carbon on soil water retention, *Geoderma*, *116*, 61–76.

Regalado, C. M., and A. Ritter (2009), A soil water repellency empirical model, *Vadose Zone J.*, *8*, 136–141.

Reynolds, W. D., and D. E. Elrick (2002), Constant head soil core (tank) method, in *Methods of Soil Analysis, Part 4–Physical Methods, Soil Science Society of America Book Series No. 5*, edited by J. H. Dane and G. C. Topp, pp. 804–808, Soil Science Society of America, Madison, WI.

Riley, H. C. F. (1979), Relationship between soil moisture holding properties and soil texture, organic matter content, and bulk density, *Agric. Res. Exp.*, *30*, 379–398.

Robichaud, P. R., J. L. Meyers, and D. G. Neary (2000), Evaluating the effectiveness of postfire rehabilitation treatments, *Gen. Tech. Rep. RMRS-GTR-63*, 85 p., United States Department of Agriculture, Forest Service, Rocky Mountain Research Station.

Rossi, C., and J. R. Nimmo (1994), Modeling of soil water retention from saturation to oven dryness, *Water Resour. Res.*, *30*, 701–708.

Rubin, J., and R. Steinhardt (1962), Soil water relations during rain infiltration: I. Theory, *Soil Sci. Soc. Am. J.*, *27*, 246–251.

Shakesby, R. A., and S. H. Doerr (2006), Wildfire as a hydrological and geomorphological agent, *Earth-Sci. Rev.*, *74*, 269–307, doi:10.1016/j.earscirev.2005.10.006.

Smith, H. G., G. J. Sheridan, P. N. J. Lane, P. Nyman, and S. Haydon (2011), Wildfire effects on water quality in forest catchments, A review with implications for water supply, *J. Hydrol.*, *396*, 170–192.

Smith, R. E., and R. H. B. Hebbert (1979), A Monte Carlo analysis of the hydrologic effects of spatial variability of infiltration, *Water Resour. Res.*, *15*, 419–429.

Snider, L. (2010), Hot, dry August set stage for Fourmile Fire, 14 Sep. 2010. http://www.dailycamera.com/fourmile-canyon-fire/ci_16067342#ixzz18nSU091W (verified 21 Dec. 2010), Boulder Daily Camera, Boulder, CO.

Soto, B., R. Basanta, and F. Diaz-Fierros (1993), Influence of wildland fire on surface runoff from a hillslope, *Acta Geolog. Hispan.*, *28*, 95–102.

Topp, G. C., and P. A. Ferré (2002), Methods for measurement of soil water content: Thermogravimetric using convective oven-drying, in *Methods of Soil Analysis. Part 4 Physical Methods, Soil Science Society of America Book Series: 5*, edited by, J. H. Dane and G. C. Topp, pp. 422–424, Soil Science Society of America, Madison, WI.

Tromp-Van Meerveld, H. J., and J. J. McDonnell (2006a), Threshold relations in subsurface stormflow: 1. A 147-storm analysis of the panola hillslope, *Water Resour. Res.*, *42*, W02410, doi:10.1029/2004WR003778.

Tromp-Van Meerveld, H. J., and J. J. McDonnell (2006b), Threshold relations in subsurface stormflow: 2. The fill and spill hypothesis, *Water Resour. Res.*, *42*, W02411, doi:10.1029/2004WR003800.

Ulery, A. L., R. C. Graham, and C. Amrhein (1993), Wood-ash composition and soil pH following intense burning, *Soil Sci.*, *156*, 358–364.

United States Department of Agriculture (USDA) (2010), Soil Survey Staff, Natural Resource Conservation Service, Web Soil Survey, [Data available at http://websoilsurvey.nrcs.usda.gov/], USDA, Washington, D.C.

Vandervaere, J. P., M. Vauclin, and D. E. Elrick (2000), Transient flow from tension infiltrometers: II. Four methods to determine sorptivity and conductivity, *Soil Sci. Soc. Am. J.*, *64*, 1272–1284.

van Genuchten, M. T. (1980), A. closed-form equation for predicting the hydraulic conductivity of unsaturated soil, *Soil Sci. Soc. Am. J.*, *44*, 892–898.

van Genuchten, M. T., F. J. Leij, and S. R. Yates (1991), The RETC code for quantifying the hydraulic functions of unsaturated soils, *EPA/600/2091/065*, Robert S. Kerr Environmental Research Laboratory, Office of Research and Development, U.S. Environmental Protection Agency, Ada, OK.

Westerling, A. L., H. G. Hidalgo, D. R. Cayan, and T. W. Swetnam (2006), Warming and earlier spring increase Western U.S. Forest Wildfire Activity, *Science*, *313*, 940–943, doi:10.1126/science.1128834.

Woods, S. W., and V. Balfour (2008), Effect of ash on runoff and erosion after a severe forest wildfire, Montana, USA, *Int. J. Wildland Fire*, *17*, 1–14, doi:10.1071/WF07040.

Woods, S. W., and V. N. Balfour (2010), The effects of soil texture and ash thickness on the post-fire hydrological response from ash covered soils, *J. Hydrol.*, *393*, 274–286, doi:10.1016/j.jhydrol.2010.08.025.

Zavala, L. M., A. Jordán, J. Gil, N. Bellinfante, and C. Pain (2009), Intact ash and charred litter reduces susceptibility to rain splash erosion post-wildfire, *Earth Surf. Processes Landforms*, *34*, 1522–1532.

Zehe, E., and G. Blöschl (2004), Predictability of hydrologic response at the plot and catchment scales: Role of initial conditions, *Water Resour. Res.*, *40*, W10202, doi:10.1029/2003WR002869.

B. A. Ebel, D. A. Martin, and J. A. Moody, U.S. Geological Survey, National Research Program, 3215 Marine St., Ste. E-127, Boulder, CO 80303, USA. (bebel@usgs.gov)